

1 **Influence of site response and focal mechanism on predictive performance**
2 **of peak ground motion prediction equations for the Greek region**

3
4 **Vincenzo Del Gaudio^{a*}, Pierpaolo Pierri^a, and Konstantinos Chousianitis^b**

5
6 *^a Dipartimento di Scienze della Terra e Geoambientali, Università degli Studi di Bari “Aldo*
7 *Moro”, Campus, via E. Orabona 4, 70125 Bari, Italy.*

8 *^b Institute of Geodynamics, National Observatory of Athens, Lofos Nymfon, 11810 Athens,*
9 *Greece*

10 ** Corresponding author - e-mail address: vincenzo.delgaudio@uniba.it*

11 *e-mail address of co-authors: pierpaolo.pierri@uniba.it; chousianitis@noa.gr*

12
13 The predictive performance of ground motion prediction equations relative to peak horizontal
14 acceleration (PHA) defined for the Greek region were found not to benefit from the inclusion of
15 terms accounting for site response. This is in part due to an inadequacy of standard methods for
16 site classification to evaluate the expected amount of PHA amplification. Indeed, the adoption of
17 a new method to derive classification from the analysis of regression residuals seems able to
18 improve the predictive performance. However, this improvement is limited by an intrinsic
19 drawback of classification criteria, i.e. the implicit assumption that amplification be a site-
20 specific property not depending on event characteristics. Instead, the inclusion of focal
21 mechanism among the explanatory variables of equations both for PHA and for peak horizontal
22 velocity (PHV) does not improve the predictive performances independently on how fault styles
23 are categorized.

24
25 **KEYWORDS**

26
27 Ground Motion Prediction Equations; Peak Horizontal Acceleration; Peak Horizontal Velocity;
28 focal mechanism; site classification; seismic hazard assessment.

29
30 **Declarations of interest:** none

1 INTRODUCTION

Empirical equations for ground motion prediction (GMPE) have several employments. They are used to quickly outline the impact of an earthquake in the first minutes of a seismic crisis, to define scenarios of future events expected within emergency preparedness planning and comprise one of the basic tools in the practice of probabilistic seismic hazard evaluation for long-term risk reduction policy. While the first equations proposed in literature had simple functional forms, which provided just a median estimate of basic ground motion parameters as function of source size and distance, in last decades considerable efforts have been addressed to refine prediction capacity adding explanatory variables and adopting more complex functional forms, also benefitting from the increasing availability of accelerometer data.

A debated question about such empirical equations is their areal validity: in principle, regional differences of seismic shakings could be observed, depending on source properties controlled by the tectonic regime and on wave propagation efficiency controlled by geological factors. These considerations motivated the introduction of regionalized equations derived from data acquired within restricted geographical areas, despite the doubts raised about its real need, considering, on the one hand, the resulting limitation of datasets used for regression and, on the other hand, the uncertain significance of inter-regional variability in comparison to the intra-regional one (cf. [1]).

The effectiveness of GMPEs depends on the accuracy of predictions of shakings for future events. Thus, an objective evaluation of whether the adoption of new more complex and/or regionally differentiated equations be justified should not simply rely on their capability of better fitting database used in regression analysis. Indeed, such an improvement may not reflect a real improvement of predictive performance for future events if the adopted models are unable to catch the real major sources of observation variability.

On the basis of such considerations, an updating of GMPEs relative to several ground motion parameters for the Greek area was recently conducted by us employing new available accelerometer data [2]. Several functional forms were tested and the most effective ones were identified from their accuracy in predicting the observations of a “validation” dataset different from that used to calculate equation coefficients through regressions. Such an approach also offered the possibility to compare the effectiveness of new equations in comparison to previously published ones and to evaluate if new equations really improve GMPE predictive performance. One of the most intriguing outcome of the cited work [2] was the observation that, while for ground velocity-based equations the optimal functional forms include site effect terms, acceleration-based equations do not seem to benefit from the consideration of such effects. Furthermore, for almost all the shaking parameters considered, the prediction accuracy does not seem to improve if equations include terms to represent the influence of focal mechanism. Therefore, in the present paper, these results are re-analysed, focusing on peak ground motion parameters, i.e. peak horizontal acceleration (PHA) and velocity (PHV). After having briefly recalled the main results obtained by our previous study [2], the results of new tests aimed at giving a better insight on regression results, are presented and the implications of the analysis outcome with regard to the optimization of GMPEs employed for hazard assessment are discussed.

2 REGRESSION METHODOLOGY AND DATASETS EMPLOYED

In our previous work [2], new GMPEs for the Greek area were calculated for PHA and PHV adopting a two-stage approach [3, 4], which separates the estimation of parameters that model the influence of source properties from those representing the effect of wave propagation. This approach is aimed at countering the bias due to the uneven sampling of magnitude-distance within the regression datasets: indeed, the prevalence in such datasets of weak events recorded at short distances and strong events at long distances can lead to underestimate attenuation rates (see [5]).

In the context of defining new GMPEs for the Greek area, several functional forms were tested starting from a general equation having the form

$$\log Y = a + b M + c \log \sqrt{R^2 + h^2} + d \sqrt{R^2 + h^2} + \sum_{i=1, N} e_i s_i + \sum_{j=1, M} f_j m_j + \varepsilon_r + \varepsilon_e \quad (1)$$

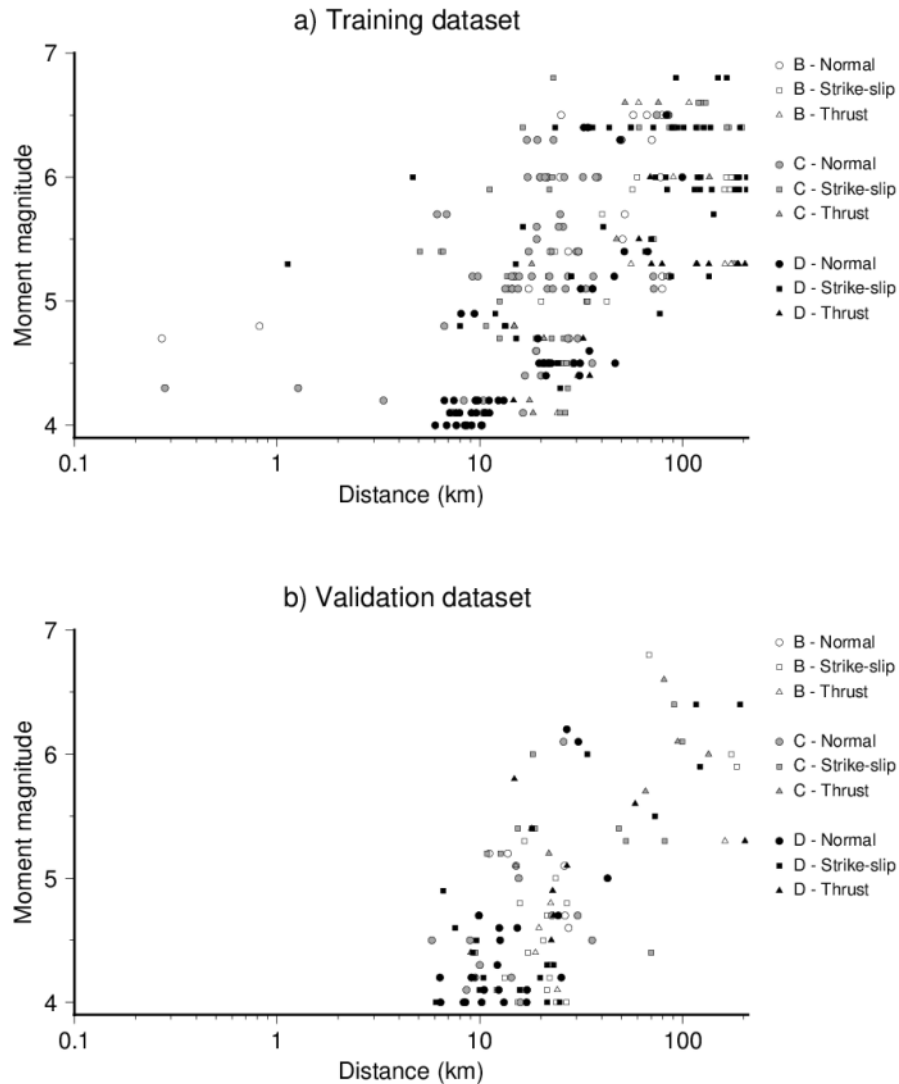
where Y is the geometric mean of orthogonal horizontal components of PHA or PHV, M is the event moment magnitude, R the epicentral distance in km, s_i and m_j are N and M dummy variables accounting for the influence of site effect and focal mechanism, respectively. The prediction uncertainties related to unmodelled intra- and inter-event variability are expressed by ε_r and ε_e , respectively. In equation (1), two causes of ground motion reduction with distance are modelled, i.e. the geometrical spreading, represented by the 3rd term, and the inelastic attenuation, represented by the 4th one, while the coefficient h accounts for the saturation effect constraining Y to finite values as R tends to 0.

All the functional forms tested in regression analyses included the first three terms of the equation (1). Alternative forms were tested excluding one or more of the other terms or varying the number of the dummy variables. Tests were carried out on a general database of accelerometer recordings of 186 events, acquired in the Greek area between 1973 and 2014 (see Table S1 in [2]). From this database, two datasets were extracted: a first “training” dataset was used to determine, through non-linear regressions, the constants appearing in equation (1) and a distinct “validation” dataset was used to compare the effectiveness of different functional forms. For the latter purpose, equations resulting from regressions were applied to predict the logarithm of ground motion observations belonging to the validation dataset and the root mean square *rmsl* of the deviations of the predicted values from the observed ones was used to rank the predictive performance of different equations.

Among the tested equations, the best predictive performances for PHA were provided by equations excluding terms for focal mechanism and site category classified according to the criteria defined by the United States National Earthquake Hazards Reduction Program (NEHRP: see [6]). With regard to PHV, the best equation was found to be the one excluding the terms for focal mechanism and inelastic attenuation, but including site effect modelled through a couple of binary variables set to (0, 0) for sites on rock (class B), (1, 0) for hard soils (class C) and (0,1) for less stiff soils (class D).

In the present paper, we investigate the reasons of these results, through a new series of tests carried out following the same approach. From the general database, two distinct “training” and “validation” datasets were extracted, the former, including 281 two-component accelerograms of 72 events recorded by 120 stations, was used for new regressions, and the latter, consisting of 112 two-component accelerograms of 109 events recorded by 44 stations, was used to compare equation predictive performances. For the requirements of the two-stage approach, the training

125 dataset was selected in such a way to include only events for which more than one recording are
 126 available. Both datasets comprise data relative to events of magnitude up to 6.8, recorded at
 127 distances up to about 200 km. Given the scarcity of short distance data in the training dataset,
 128 which implies a rather weak constraint for predictions at such distances, validation was carried
 129 out only on recordings acquired at distances longer than 5 kilometers. Figure 1 shows the
 130 magnitude/distance distribution of the recordings that form the two datasets.
 131



132
 133 *Fig. 1. Magnitude of recorded events as function of distance of the recording station for the*
 134 *“training” dataset (a), used in equation regressions, and for the “validation” dataset (b), used*
 135 *in the equation effectiveness evaluation. White, grey and black symbols are used for data*
 136 *acquired on sites of type B, C and D, respectively, whereas differences of source focal*
 137 *mechanisms are marked by symbol shape (circle = normal; square = strike-slip; triangle =*
 138 *thrust).*

139

140 3 DATA ANALYSIS

141

142 The outcome of regressions carried out in [2] raised questions that stimulated a deeper analysis
143 with the support of additional tests to get a better insight on the result implications. The two main
144 questions were i) the different effectiveness of the introduction of terms accounting for site
145 response in equations for PHA and PHV and ii) the lack of improvement in predictions provided
146 by equations including terms to represent the influence of focal mechanism. Here, we re-examine
147 these results through a more detailed analysis of residuals of equations derived for PHA and
148 PHV.

149

150 3.1 Site Effect

151

152 The main difference between the equation forms that provided the best predictive performance
153 for PHA and PHV (evaluated from the minimization of root mean square of residuals *rmsl*
154 calculated on the validation dataset) is that, while the inclusion of terms representing site
155 conditions improves significantly the GMPE predictions for PHV, the same does not happen for
156 PHA. This is true not only for the best equation obtained for each ground motion parameter.
157 Indeed, ordering equations by increasing values of *rmsl*, site class is present in the seven best
158 GMPEs for PHV but not in the two best equations for PHA. Furthermore, any PHA equation
159 including site effect terms gives a worse performance than that with the same functional form but
160 without site terms and the use of a single variable distinguishing rock from soil sites gives better
161 results than the use of two variables distinguishing also between more or less stiff soils (see
162 Table S2 in [2]).

163 At present, the sites of the Greek accelerometer stations are classified according to the NEHRP
164 criteria, based on the mean velocity of shear waves in the top 30 meter of soil (V_{S30}). This
165 parameter shows some correlation with site conditions responsible for resonance phenomena,
166 even though, the use of this parameter alone for site response characterization presents limits and
167 drawbacks (cf. [7]). Additionally, it can be observed that PHV reflects better than PHA the
168 shaking properties responsible for damaging effects (cf. [8]). Indeed, high PHA values for short-
169 duration high-frequency shakings typically do not produce significant damages on engineering
170 structures, whereas PHV, deriving from an integration of ground acceleration, tends to reach
171 higher values for longer and relatively lower-frequency shakings, responsible for more severe
172 damages.

173 These considerations suggest the possible need of using distinct site classification criteria to be
174 used for equations predicting PHA and PHV values. Thus, we experimented a reclassification of
175 stations of the Greek accelerometer network, aimed at improving the prediction of the site effect
176 influence on PHA values. This reclassification was based on a cluster analysis of regression
177 residuals aimed at grouping the station sites into a number of distinct classes. Such an approach
178 relies on the consideration that ground motions observed for given magnitudes and distances
179 should differ from median values predicted by a GMPE that does not consider site effect by
180 amount depending on site amplification. Thus, large positive residuals can be expected at sites
181 affected by resonance phenomena (e.g. on soft soils) and negative ones at sites not affected by
182 amplification (e.g. on compact rocks).

183 The method we propose consists of using preliminarily a GMPE not including site effect terms to
184 calculate median ground motion expected for magnitudes and epicentral distances corresponding

185 to those of events recorded by accelerometer stations. Only stations are selected for which two or
 186 more recordings are available and the average of residuals is calculated for each of these stations.
 187 They are then ordered by increasing values of average and the optimal grouping into classes is
 188 obtained by looking for the class limits that minimize the root mean square of deviations of
 189 residuals of each recording from the average of residuals of stations belonging to the same class
 190 of the recording station.

191 In order to compare the predictive performance of equations excluding site effect terms with
 192 those including site response classified according to both the NEHRP criteria and the new
 193 approach, regressions were carried out for each equation on a subset of the training dataset of
 194 Fig. 1a, comprising only stations for which more than one recording are available. This subset
 195 includes 220 two-component recordings acquired by 63 stations for 59 events. The equation
 196 obtained with the functional form excluding site response terms is

$$197 \log PHA = 0.410 + 0.513 M - 0.896 \log \sqrt{R^2 + 5.002^2} - 0.0054 \sqrt{R^2 + 5.002^2} \pm 0.265 \quad (2),$$

199 where 0.265 is the total standard deviation estimated, given by the quadratic mean of ε_r and ε_s .
 200 With regard to equations including site classes, all stations in the training dataset are classified in
 201 one of three NEHRP classes (B - rock, C – hard soil and D – relatively softer soil). Thus, two
 202 dummy variables s_C and s_D were used to distinguish among the three categories, setting them to
 203 (0, 0), (1, 0) and (0, 1) for site class B, C and D, respectively. Using the NEHRP criteria to
 204 assign the accelerometer sites to the three classes, the resulting equation is:

$$205 \log PHA = 0.171 + 0.524 M - 0.921 \log \sqrt{R^2 + 4.941^2} - 0.0051 \sqrt{R^2 + 4.941^2}$$

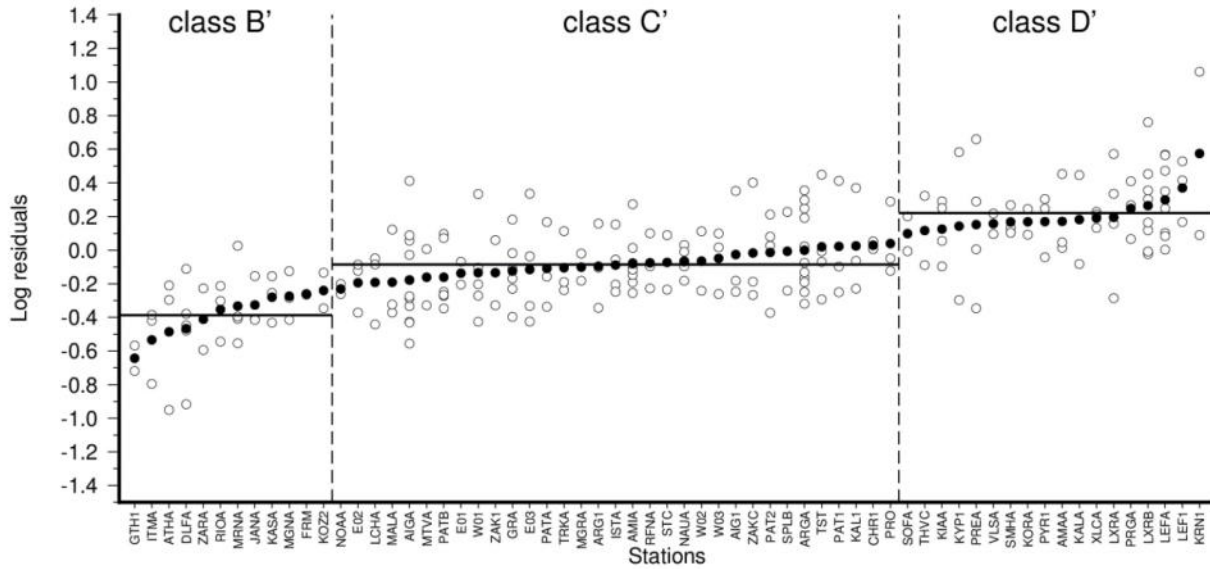
$$206 + 0.191 \cdot s_C + 0.251 s_D \pm 0.251$$

207 (3)

208
 209
 210 The residuals of the regression provided by equation (2) were used to reclassify the station sites
 211 into three classes B', C' and D'. Figure 2 shows the residuals distribution and the site class
 212 grouping obtained from the cluster analysis, whereas Tab. 1 reports a comparison between the
 213 original classification (based on the NEHRP criteria) and that resulting from the cluster analysis.
 214 The three classes are characterized by mean residuals equal to -0.387 ± 0.222 (class B), $-$
 215 0.086 ± 0.220 (class C) and 0.220 ± 0.257 , which are results consistent with the expected increase
 216 of ground motion passing from rock site to more and less stiff soils.

217 In Table 1, in order to highlight classification differences, cell reporting classes with different
 218 ranking in terms of expected amplification level are marked with different grey shades (from
 219 white for B/ B' to dark grey for D/D'). One can notice that the new classification agrees with the
 220 NEHRP one only for about half of the stations examined (33 out of 63). For 25 sites, the
 221 reclassification moves the site by one level above or below that of the NEHRP class. In some
 222 cases, this can depend on a slight shift of the class limit (e.g. KOZ2 and NOAA, which
 223 exchanges their belonging to rock and stiffer soil classes in the old and new classification, are
 224 both located close to the boundary between class B' and C'). However, in some other cases, the
 225 observed residuals are inconsistent with the NEHRP classification (e.g. E02 and LCHA, which
 226 NEHRP criteria assign to class D, show residuals near the limit between class B' and C'), and in
 227 five cases (FRM, KYP1, RIOA, VLSA and ZARA) classification varies by two levels (from B to
 228 D' or from D to B').

229
 230



231 *Fig. 2. Results of the site reclassification based on the residuals of the regression of PHA values*
 232 *according to the equation (2). Open circles represent residuals of single recordings at each*
 233 *station of the training dataset, black dots correspond to the mean value of residuals for each*
 234 *station, vertical dashed lines separate the stations classified in different site classes and*
 235 *horizontal solid lines mark the average of residuals for the stations of each site class.*

236
 237 Using the new station classification, a new equation was calculated by regression on the same
 238 dataset, adopting a functional form where site classes are expressed through two dummy
 239 variables s_C and s_D . The result is:

$$\log PHA = 0.097 + 0.481 M - 0.763 \log \sqrt{R^2 + 4.686^2} - 0.0058 \sqrt{R^2 + 4.686^2} + 0.263 \cdot s_C + 0.531 s_D \pm 0.190$$

243 (4),

244
 245 which is characterized by a considerable lower standard deviation than the previous equations.
 246 This was expected, because the new classification is correlated to residuals of equation (2) better
 247 than the classification used in equation (3), so that equation (4) can explain in terms of site
 248 response a larger amount of the observed ground motion variability.

249 In order to verify if the reduction of standard deviation is due to a real improvement of the
 250 predictive performance and not just to an “overfitting” of the dataset used for regressions, the
 251 predictions of the three equations were compared with the observations of a different dataset.
 252 This consists of a subset of the validation dataset of Fig. 1b, including only recordings acquired
 253 at the sites for which the cluster analysis provided the new classification, i.e., 88 recordings
 254 acquired by 24 stations for 86 events. Applied to these data, the three equation provides
 255 estimated errors whose root mean square *rmsl* (calculated on the logarithm of PHA) was found
 256 0.299 for equation (2), 0.321 for equation (3) and 0.287 for equation (4).

257
 258

259 *Table 1. Comparison between accelerometer site classes derived from the NEHRP criteria and*
 260 *from a reclassification based on cluster analysis. For each station, geographic coordinates and*
 261 *the available number of recordings are reported.*

262

Code	Lat	Lon	N. rec	NEHRP	Reclass	Code	Lat	Lon	N. rec	NEHRP	Reclass
AIG1	38.250	22.067	3	C	C'	MGNA	38.656	20.791	3	B	B'
AIGA	38.251	22.085	11	C	C'	MGRA	37.996	23.345	2	C	C'
AMAA	37.795	21.350	3	D	D'	MRNA	38.525	22.117	4	C	B'
AMIA	38.528	22.378	8	C	C'	MTVA	39.770	21.183	2	D	C'
ARG1	38.167	20.483	3	C	C'	NAUA	38.394	21.833	5	B	C'
ARGA	38.177	20.479	11	C	C'	NOAA	37.973	23.718	2	B	C'
ATHA	38.001	23.774	3	C	B'	PAT1	38.250	21.733	3	C	C'
CHR1	40.133	21.733	2	C	C'	PAT2	38.238	21.738	4	C	C'
DLFA	38.478	22.496	5	B	B'	PATA	38.250	21.730	3	C	C'
E01	40.671	23.307	2	D	C'	PATB	38.239	21.727	6	D	C'
E02	40.674	23.316	3	D	C'	PREA	38.956	20.753	4	C	D'
E03	40.676	23.324	4	D	C'	PRGA	39.286	20.402	3	D	D'
FRM	40.655	23.298	2	D	B'	PRO	40.688	23.276	3	C	C'
GRA	40.675	23.289	6	D	C'	PYR1	37.670	21.438	3	D	D'
GTH1	36.754	22.567	2	B	B'	RFNA	38.020	23.987	3	C	C'
ISTA	38.953	23.155	4	D	C'	RIOA	38.296	21.791	3	D	B'
ITMA	37.178	21.925	3	B	B'	SMHA	38.251	20.648	3	C	D'
JANA	39.656	20.849	3	B	B'	SOFA	39.338	22.097	2	D	D'
KAL1	37.033	22.100	3	C	C'	SPLB	38.004	23.710	2	C	C'
KALA	37.030	22.120	2	C	D'	STC	40.649	23.305	2	C	C'
KASA	39.746	19.936	3	B	B'	THVC	38.319	23.318	2	C	D'
KIAA	38.014	22.750	4	D	D'	TRKA	39.553	21.766	3	D	C'
KORA	37.939	22.931	2	D	D'	TST	40.664	23.291	4	D	C'
KOZ2	40.300	21.790	2	C	B'	VLSA	38.177	20.589	2	B	D'
KRN1	36.802	21.961	2	C	D'	W01	40.665	23.274	5	D	C'
KYP1	37.250	21.667	2	B	D'	W02	40.661	23.260	2	D	C'
LCHA	37.938	21.264	3	D	C'	W03	40.660	23.251	3	D	C'
LEF1	38.826	20.702	3	D	D'	XLCA	38.078	22.631	3	D	D'
LEFA	38.833	20.704	8	D	D'	ZAK1	37.784	20.898	2	D	C'
LXRA	38.200	20.437	4	D	D'	ZAKC	37.784	20.898	3	D	C'
LXRB	38.200	20.437	8	D	D'	ZARA	37.487	21.649	2	D	B'
MALA	38.622	23.232	3	C	C'						

263

264

265 It is noteworthy that the *rmsl* calculated on the regression dataset was found equal to 0.307,
 266 0.292 and 0.236, for (2), (3) and (4), respectively. Thus, equation (3), which adopts the NEHRP
 267 classification, while, in comparison to equation (2), slightly improves the fitting with the

268 regression dataset, shows a worse performance in predicting the observations of the validation
269 dataset. This result is consistent with what was observed in [2], and confirms that the reduction
270 of standard deviation depends only on an “overfitting” of data, without providing an
271 improvement of prediction accuracy on independent data. On the other hand, in comparison to
272 the basic equation (2), the equation (4), which adopts the new classification, shows an
273 improvement of prediction accuracy, which is however much smaller than that observed when
274 applied to the regression dataset. This suggests that the improvement obtained in PHA prediction
275 with a classification more specific for this parameter is rather weak.

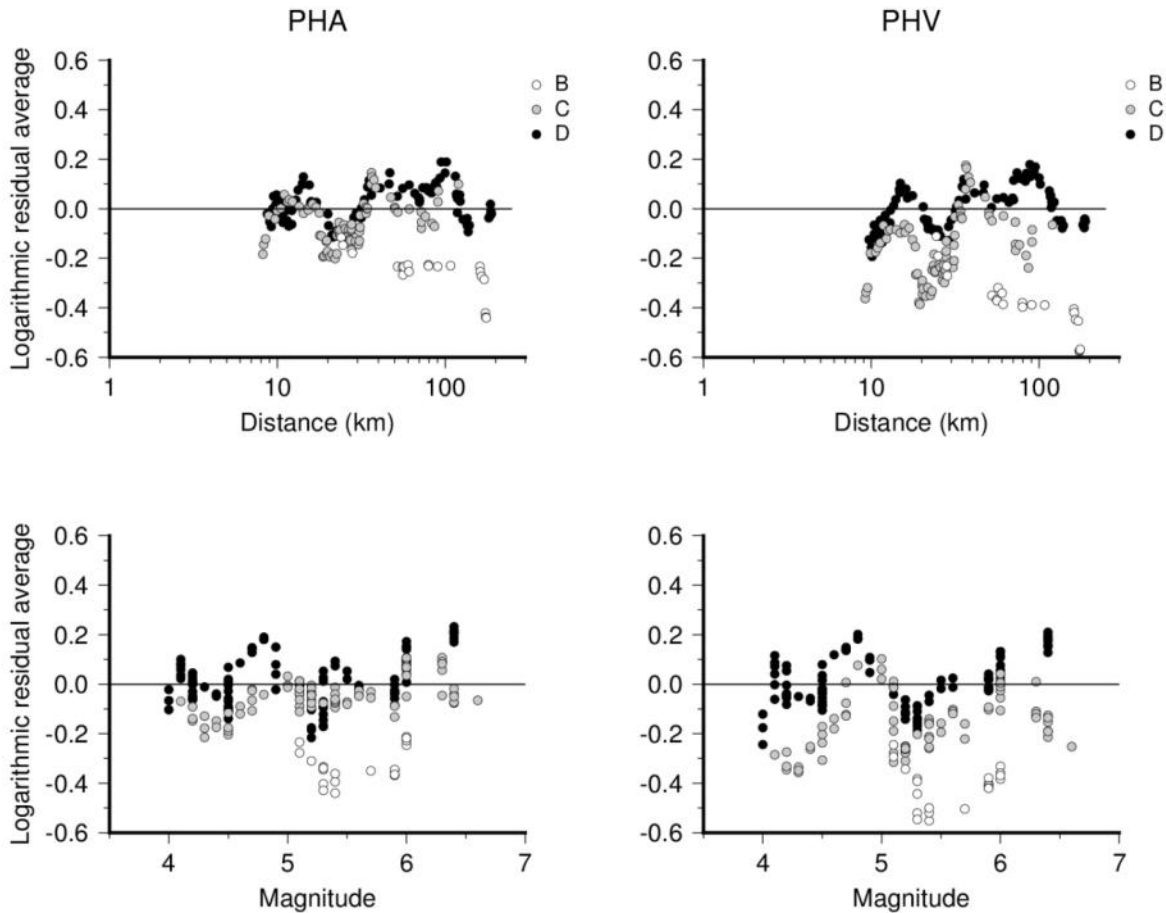
276 A possible explanation of the limited efficacy of the inclusion of site class as explanatory
277 variable is the implicit assumption of common GMPEs that site amplification, apart from
278 fluctuations related to casual factors (e.g. seismic wave incidence angle at the surface) is a site-
279 specific property independent on seismic source properties. Indeed, its modelling with binary
280 dummy variables implies that the amplification amount is on average the same for any event of
281 different magnitude and distance. However, experimental observations indicate that
282 amplification may not be independent on source size and distance, because these factors
283 influence the spectral distribution of shaking energy, which generates a different response
284 according to the site resonance frequency. It was observed, for instance (see [9]), that, in case of
285 events of magnitude and distance below a certain threshold, PHA at reference sites on rock can
286 be even larger than on nearby sites on soil known to be affected by amplification. This is likely
287 due to a major concentration of seismic shaking energy, for low-magnitude short-distance events,
288 at frequencies that are higher than those of soil site resonance and are more efficiently
289 transmitted through rock materials.

290 Therefore, to investigate the reason of the limited effectiveness of site class for the prediction of
291 PHA, we examined how residuals of GMPE excluding site terms vary with distance and
292 magnitude for site classified according to the NEHRP criteria. Figure 3 (left side) shows the
293 results of this analysis applied to the residuals of the regression of equation (2). A running
294 average was calculated over the residuals of 11 consecutive observations of the regression
295 dataset ordered by increasing distance (top) and magnitude (bottom), so to reduce the influence
296 of fluctuations related to other factors that can randomly influence the results. It is apparent that
297 residuals do not show significant systematic differences between sites classified into NEHRP
298 classes C and D, whereas sites of class B shows, as expected, PHA values below the average and
299 clearly smaller than sites C and D, but only at distances larger than 30 km and magnitudes over
300 5.2. This indicate that at short distances from moderate magnitude events, sites classified into
301 classes B, C and D do not show significant differences of the PHA amplification factor. The
302 same occurs for any distance and magnitude for sites of class C and D, which additionally
303 explains the mentioned observation that equations including two dummy variables were found
304 not to perform better than those using just one variable for site classification.

305 For comparison, a similar analysis was carried out also on the PHV values of the same dataset. A
306 regression was performed using a functional form without site class term and without inelastic
307 attenuation term (which according to the results of the previous study², was found to have a
308 negligible influence on PHV prediction accuracy). The resulting equation is

$$310 \log PHV = -1.064 + 0.681 M - 1.459 \log \sqrt{R^2 + 6.606^2} \pm 0.290 \quad (5),$$

311
312 and the running averages of residuals as function of distance and magnitude are reported in the
313 right part of Fig. 3.



315
 316 *Fig. 3. Running averages of logarithmic residuals of GMPE not including site class term, as*
 317 *function of distance (top) and magnitude (bottom), for peak acceleration (left) and velocity*
 318 *(right). Data relative to different site classes are represented with different grey shade,*
 319 *according to the legend.*

320

321

322 One can notice that, for PHV, residuals relative to sites of class C are prevailingly quite below
 323 those of sites D and those of sites B below those of both of them, even though, as for PHA,
 324 differences between sites B and C tends to reduce for distances shorter than 30 km and
 325 magnitude smaller than 5.2. Overall, the distribution of residuals for PHV estimations appears
 326 more consistent with the expected increase of ground motion passing from a rock site to a hard
 327 soil and to a less stiff ground. This can explain why GMPEs for peak velocity seem to benefit
 328 more from the introduction of a representation of site conditions through two variables. A similar
 329 result had been previously obtained for GMPE predicting Arias intensity [10], which supported
 330 the reliability of the existing site classification for ground motion parameter related to the total
 331 shaking energy.

332 These results, however, indicate also that the site classification based on residual analysis can be
 333 influenced by the combination of magnitude and distances that are prevailing for the recordings
 334 of a given station. For instance, a site on rock reporting recordings only for short-distance/lower-
 335 magnitude events, will show residuals comparable with those observed for sites on soil, and

336 could then be classified together to them. Thus for generic predictions of PHA, the distinction
 337 between site classes does not seem useful, unless new kind of site effect modelling be introduced
 338 assuming this effect as depending on magnitude/distance combinations (which, however, would
 339 require a larger amount of data for regressions).

340

341 **3.2 Focal Mechanism**

342

343 A second question examined is the apparent insignificance of focal mechanism as explanatory
 344 variable, which implies that, according to the comparative tests carried out on the validation
 345 dataset, fault mechanism is not a factor that needs to be taken into account for prediction
 346 optimization. We carried out some additional tests to verify if this result could depend on an
 347 inadequate association of focal mechanisms to dummy variables. In our previous work [2], the
 348 categorization of event focal mechanisms had been simplified unifying strike-slip and thrust fault
 349 types, following the outcome of previous studies [11], thus a single dummy variable m had been
 350 included in equation (1), setting its value to 0 for normal faults and to 1 otherwise. Therefore, we
 351 carried out new regressions on the entire training dataset of Fig. 1a. In a first regression we used
 352 again a single dummy variable, named m_T , but set to 1 for thrust faults and to 0 otherwise,
 353 whereas in a second regression the three basic mechanism types were separated by using two
 354 dummy variables m_S and m_T , set to (0,0), (1,0) and (0,1) for normal, strike-slip and thrust
 355 mechanisms, respectively. For comparison homogeneity, the same dataset was used also to
 356 recalculate equations without focal mechanism terms and with a single dummy variable m_{ST} , set
 357 to 0 for normal faults and to 1 otherwise (as in [2]).

358 The equations resulting from regressions are, for PHA:

359

$$360 \log PHA = 0.396 + 0.522 M - 0.952 \log \sqrt{R^2 + 5.379^2} - 0.0047 \sqrt{R^2 + 5.379^2} \pm 0.262 \quad (6)$$

361

$$362 \log PHA = 0.420 + 0.499 M - 0.952 \log \sqrt{R^2 + 5.379^2} - 0.0047 \sqrt{R^2 + 5.379^2}$$

$$363 \quad + 0.236 m_{ST} \pm 0.255$$

364 (7)

365

$$366 \log PHA = 0.364 + 0.531 M - 0.952 \log \sqrt{R^2 + 5.379^2} - 0.0047 \sqrt{R^2 + 5.379^2}$$

$$367 \quad + 0.246 m_T \pm 0.259$$

368 (8)

369

$$370 \log PHA = 0.402 + 0.507 M - 0.952 \log \sqrt{R^2 + 5.379^2} - 0.0047 \sqrt{R^2 + 5.379^2}$$

$$371 \quad + 0.203 \cdot m_S + 0.326 m_T \pm 0.255$$

372 (9).

373

374 Taking into account the results reported in the previous section about the significant influence of
 375 site effects for the prediction of PHV, test relative to this parameter were carried out adopting a
 376 functional form including the dummy variables s_C and s_D to distinguish among sites of class B, C
 377 and D. Instead, following the outcome of the previous work [2] about the insignificance of
 378 inelastic attenuation, the relative term was omitted. The equations obtained by regressions are:

379

$$380 \log PHV = -1.526 + 0.710 M - 1.438 \log \sqrt{R^2 + 6.405^2} + 0.198 s_C + 0.355 s_D \pm 0.259$$

381

(10)

382 $\log PHV = -1.483 + 0.691 M - 1.438 \log \sqrt{R^2 + 6.405^2} + 0.198 s_C + 0.355 s_D$
383 $+ 0.178 m_{ST} \pm 0.256$
384 (11)

385
386 $\log PHV = -1.591 + 0.720 M - 1.438 \log \sqrt{R^2 + 6.405^2} + 0.198 s_C + 0.355 s_D$
387 $+ 0.275 m_T \pm 0.256$
388 (12)

389
390 $\log PHV = -1.545 + 0.705 M - 1.438 \log \sqrt{R^2 + 6.405^2} + 0.198 s_C + 0.355 s_D + 0.123 m_S$
391 $+ 0.326 m_T \pm 0.255$
392 (13).

393
394 One can notice that the coefficients of terms accounting for attenuation (geometric or inelastic)
395 and site effect (when present) are the same for all the equations relative to the same ground
396 motion parameter. This is a consequence of the two-stage approach, since the coefficients of
397 these terms are all calculated in the first stage, which is independent from source properties. On
398 the contrary, the other coefficients, depending on magnitude and focal mechanism, differ
399 because are calculated in the second stage by using regression equations of different form.
400 Despite the slightly lower value of regression standard deviation for equations that include focal
401 mechanism terms, when these equations are applied to the entire validation dataset of Fig. 1b, the
402 resulting root mean square of logarithmic errors (*rmsl*) is higher. With regard to PHA, for
403 equation (6) the resulting *rmsl* is 0.305, against 0.315 for (7), 0.309 for (8) and 0.317 for (9). For
404 PHV, the equation (10) gives *rmsl* = 0.317, whereas equations (11), (12) and (13) give 0.342,
405 0.324 and 0.340, respectively. Both for PHA and PHV, the distinction of thrust faults alone
406 (equations 8 and 12) from the other types seems to give better predictions than other mechanism
407 combinations, but, in any case, these predictions are worse than those obtained totally neglecting
408 the fault type influence.

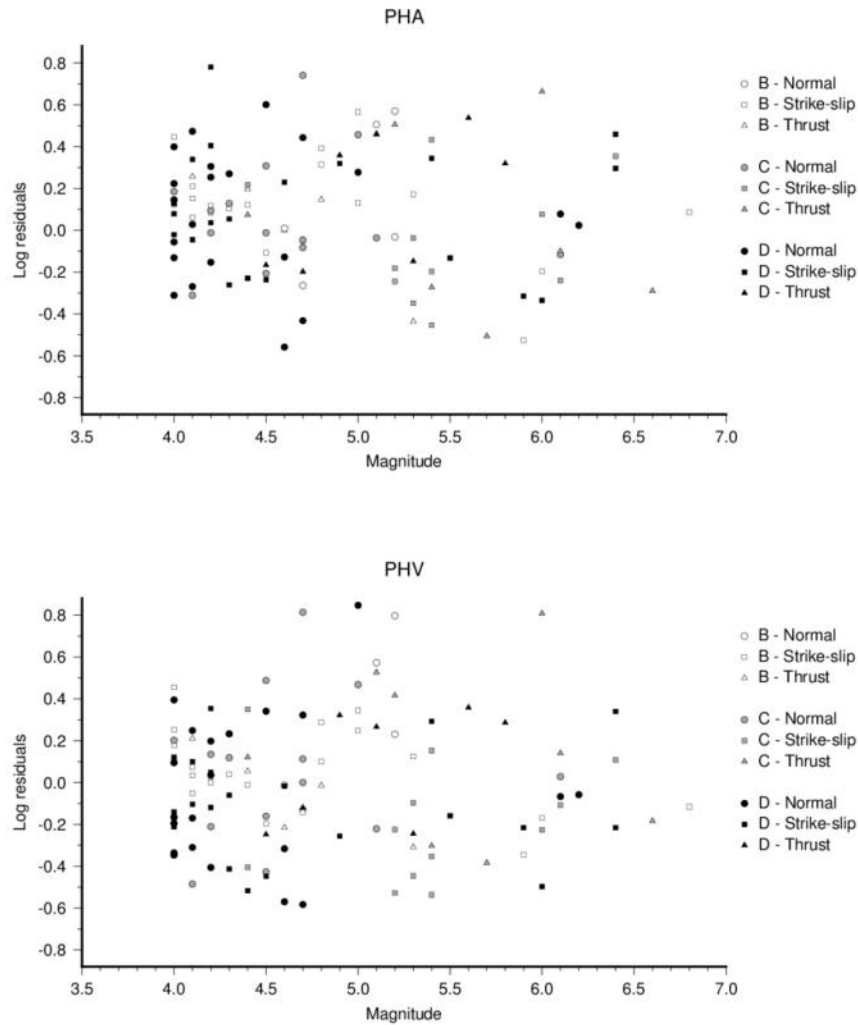
409 The absence of any improvement with the inclusion of focal mechanism among the explanatory
410 variable reflects the absence of any correlation between the mechanisms of the recorded events
411 and the residuals of observations obtained from the equations not including focal mechanism
412 terms. Figure 4 shows that, for different events of different magnitude, one can find large
413 residuals both positive and negative for the same fault type, without any preferential
414 concentration around a mean level changing from one mechanism to the other, also taking into
415 account the possible different influence of site effects on the ground motion recording.
416 This is confirmed also using the best equations obtained in the previous study [2] to calculate the
417 PHA and PHV values of the validation dataset. Examining the averages of residuals relative to
418 recordings acquired under similar site conditions for events of different source type (Fig. 5), no
419 systematic variation is recognizable passing from normal to strike-slip or thrust fault
420 mechanisms. Although, based on this test alone, one cannot exclude that such a result can
421 depends on an incorrect station site classification, the results of the tests reported in section 3.1
422 about site effect influence let us exclude such an explanation at least for PHV. Thus, data
423 indicate that, within the magnitude interval covered by the regression dataset (from 4.0 to 6.8),
424 the employment of focal mechanism as explanatory variable to predict peak ground motion
425 parameters for the Greek area does not seem justified, and the influence of source properties can
426 be represented by magnitude alone.

427

428
429
430
431
432
433
434
435
436
437
438
439
440
441

4 DISCUSSION AND CONCLUSION

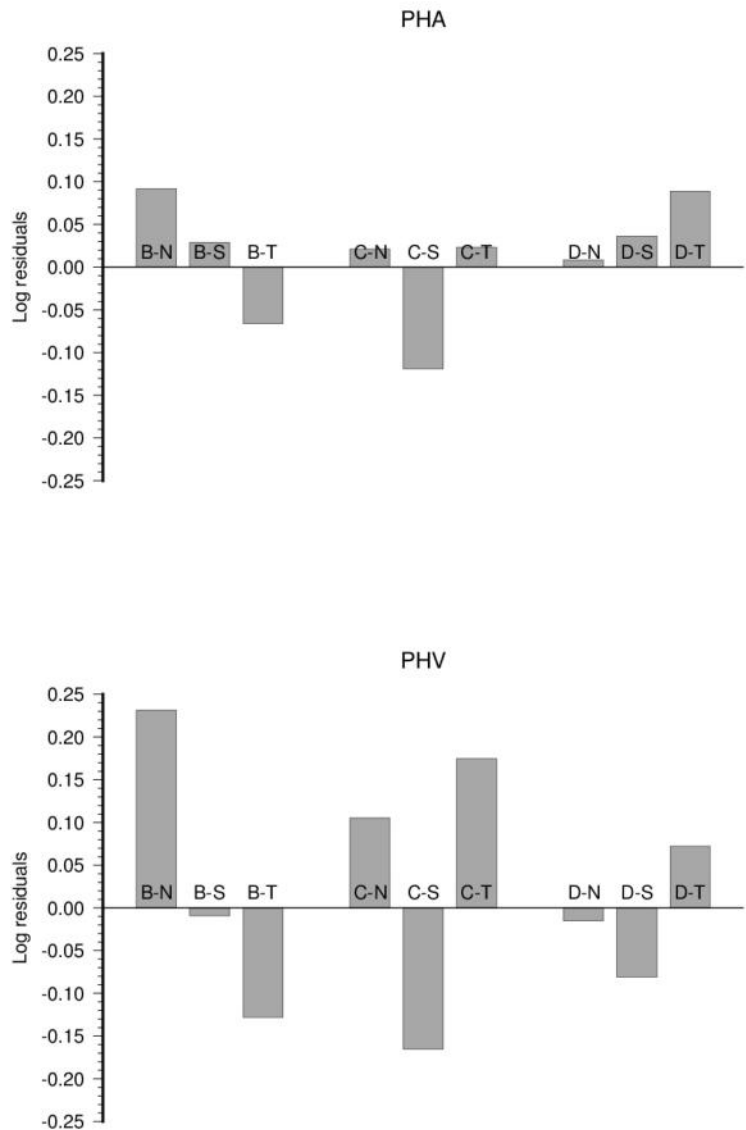
The results of data analysis reported in previous sections have some implications about the use of GMPE in hazard assessment, especially when aimed at providing elements required for the definition of building codes in seismic regions. According to a generally recommended practice, the definition of design spectrum for elastic analysis is anchored to the results of a “base” hazard assessment, expressed in terms of design ground acceleration (DGA). This parameter is given by the PHA value with a defined exceedance probability calculated at sites where the presence of outcropping compact rocks is assumed (e.g. site of class A, according to the Eurocode 8: see [12]). The consideration of the real local site conditions is subsequently taken into account by calculating the increase of seismic actions due to site response, either through simplified methods, as reported in [12], or through numerical modelling.



442
443
444
445
446

Fig. 4 Residuals of the application of the equations (6) and (10) (excluding focal mechanism) to predict PHA (top) and PHV (bottom) values of the validation dataset. Data relative to recordings of events with different focal mechanism, acquired at sites of different type, are represented through different symbols and grey shades, according to the legend.

447
448



449
450
451
452
453
454
455
456
457

Fig. 5 Averages of logarithmic residuals derived applying the best equations obtained by [2] to predict PHA (top) and PHV (bottom) values of the validation dataset. Data relative to recordings of events with different focal mechanism, acquired at sites of different type are labelled with B, C and D (indicating the site class of the recording stations), followed by N, S and T, for normal, strike-slip and thrust mechanisms, respectively.

458 Therefore, for the calculations of DGA, once the probability of earthquake occurrence has been
459 evaluated for seismic events occurring within relevant seismogenic zones, a GMPE is used to
460 estimate the probability distribution of ground motion expected at sites on rock. For this purpose,
461 GMPE calibrated on accelerometer database are generally employed, setting the site effect terms
462 to the values for rock site conditions. The results of tests shown in the present study, however,

463 suggest that GMPEs calibrated on data of accelerometer stations classified according to standard
464 criteria (e.g. based on simplified parameters like V_{S30}) might provide unreliable estimations.
465 Therefore, in assigning class to accelerometer stations whose data are to be used in GMPE
466 regressions, it is advisable to adopt criteria more specific for PHA estimates, for instance
467 following the approach outlined in section 3.1. Although such a method cannot be of general use
468 for site classification, being applicable only where accelerometer recordings are available, and
469 despite the results of classification can be influenced by the prevailing magnitude/distance
470 combination for the recordings available at different stations, stations classified as B' are in any
471 case representative of site conditions not affected by amplification. Thus, having built a database
472 for GMPE regression by using a classification based on PHA residual analysis, the use of the
473 resulting equation, once the site terms are set to the values for class B', allows estimating the
474 PHA values expected in absence of amplification, which is just what required for "base" hazard
475 assessment.

476 Another indication deriving from our study is that, for hazard assessment, it is not worthwhile
477 employing GMPEs that model the influence of focal mechanism on PHA, which, moreover,
478 require a differentiations of calculations for seismogenic zones characterized by different focal
479 mechanisms. Indeed, our tests indicate that the inclusion of fault style among the GMPE
480 explanatory variables does not improve the accuracy of PHA prediction. This consideration also
481 simplifies the use of GMPE in hazard assessment procedures that define seismicity rates without
482 the need of a preliminary identification of seismotectonic zones distinct by prevailing fault style
483 (as in [13]).

484 Overall, some main learnings can be derived from the comparative analyses of the performance
485 of ground motion prediction equations calculated for the Greek region. In the present study,
486 performance analysis was based on the examination of the distribution of residuals deriving from
487 GMPE application to a set of observations distinct from those used in regressions. Results
488 indicate that, for a generic use of prediction equations in the examined area, there is no reason
489 for using site effect terms for PHA and focal mechanism terms for both PHA and PHV, at least
490 within the range of magnitudes (4.0-6.8) and distances (up to 200 km) investigated.

491 With regard to the site effect, the ineffectiveness of its consideration for PHA estimates can be in
492 part due to a poor consistency between site classification based on the shear wave velocity of the
493 top 30 meter of soil (V_{S30}) and the relative amplification factors observed for peak horizontal
494 acceleration. Indeed, the adoption of classification criteria directly based on the PHA
495 observations, through the analysis of residuals from equations excluding site effect terms, seems
496 able to slightly improve the predictive performance of the resulting equations. However, an
497 additional factor that deteriorates the equation performance is also a possible inadequacy of site
498 amplification modelling as a purely site-specific property, regardless of event magnitude and
499 distance. Indeed the combination of these two factors controls the spectral energy distribution,
500 thus significantly modifying the site response for different events, in dependence on the site
501 resonance frequencies. Unless magnitude/distance-dependent modelling of site effect can be
502 introduced (relying on an adequate amount of data), the fairest solution is simply to make use of
503 median estimators of PHA neglecting the influence of site response.

504 With regard to the use of GMPE specifically for hazard assessment, however, there is the need of
505 defining equations specifically predicting PHA at sites on rock. For this purpose, the use of
506 database for which site classification is directly derived from the analysis of PHA residuals could
507 give equations that are better representative of site conditions unaffected by amplification,

508 according to the requirement of “base” hazard assessment, independently on the “geological”
509 correctness of classification.

510

511 **Acknowledgements**

512 This study was carried out with the financial support of Italian Ministry of Education, University
513 and Research.

514

515 **REFERENCES**

516

- 517 [1] Bommer JJ, Stafford PJ, Akkar S. Current empirical ground-motion prediction equations for
518 Europe and their application to Eurocode 8. *Bull Earthquake Eng.* 2010; 8: 5,
519 doi:10.1007/s10518-009-9122-9.
- 520 [2] Chousianitis K, Del Gaudio V, Pierri P, Tselentis GA. Regional Ground-Motion Prediction
521 Equations for amplitude-, frequency response-, and duration-based parameters for Greece.
522 *Earthquake Engng Struct Dyn.* 2018; 47: 2252–2274, doi: 10.1002/eqe.3067.
- 523 [3] Joyner WB, Boore DM. Peak horizontal acceleration and velocity from strong motion
524 records including records from the 1979 Imperial Valley, California, earthquake. *Bull*
525 *Seismol Soc Am.* 1981; 71: 2011-2038.
- 526 [4] Joyner WB, Boore DM. Methods for regression analysis of strong-motion data. *Bull Seismol*
527 *Soc Am.* 1993; 83: 469–487.
- 528 [5] Fukushima Y, Tanaka T. A new attenuation relation for peak horizontal acceleration of
529 strong earthquake ground motion in Japan. *Bull Seismol Soc Am.* 1990; 80: 757-783.
- 530 [6] BSSC (Building Seismic Safety Council). NEHRP recommended provisions for seismic
531 regulations for new buildings and other structures (FEMA 450). National Institute of
532 Building Sciences, Washington, 2003, pp. 338.
- 533 [7] Castellaro S, Mulargia F, Rossi PL. Vs30: Proxy for Seismic Amplification? *Seismol Res*
534 *Lett* 2008; 79: 540-543.
- 535 [8] Wu YM, Teng T, Shin TC, Hsiao NC. Relationship between Peak Ground Acceleration,
536 Peak Ground Velocity, and Intensity in Taiwan. *Bull Seismol Soc Am.* 2003; 93: 386-396.
- 537 [9] Del Gaudio V, Wasowski J. Advances and problems in understanding the seismic response
538 of potentially unstable slopes. *Eng Geol.* 2011; 122: 73-83.
- 539 [10] Chousianitis K, Del Gaudio V, Kalogeras I, Ganas A. Predictive model of Arias intensity
540 and Newmark displacement for regional scale evaluation of earthquake-induced landslide
541 hazard in Greece. *Soil Dyn Earthq Eng.* 2014; 65: 11-29.
- 542 [11] Danciu L, Tselentis G-A. Engineering Ground-Motion Parameters Attenuation Relationships
543 for Greece. *Bull Seismo. Soc Am.* 2007; 97(1B): 162–183.
- 544 [12] EN 1998-1. Eurocode 8: Design of structures for earthquake resistance - Part 1: General
545 rules, seismic actions and rules for buildings. European Committee for Standardization,
546 2004, pp. 229.
- 547 [13] Frankel A. Mapping Seismic Hazard in the Central and Eastern United States. *Seismol Res*
548 *Lett* 1995; 66: 8-21.

549